Mon. Not. R. Astron. Soc. **000**, 1–?? (2015) Printed 27 March 2015 (MN LATEX style file v2.2)

Energy levels, radiative rates and electron impact excitation rates for transitions in C III⋆

Kanti M. Aggarwal[1]† and Francis P. Keenan[1]
[1]*Astrophysics Research Centre, School of Mathematics and Physics, Queen's University Belfast, Belfast BT7 1NN, Northern Ireland, UK*

Accepted 2015 March 25. Received 2015 March 12; in original form 2015 February 6

ABSTRACT

We report energy levels, radiative rates (A-values) and lifetimes for the astrophysically-important Be-like ion C III. For the calculations, 166 levels belonging to the $n \leqslant 5$ configurations are considered and the GRASP (General-purpose Relativistic Atomic Structure Package) is adopted. Einstein A-coefficients are provided for all E1, E2, M1 and M2 transitions, while lifetimes are compared with available measurements as well as theoretical results, and no large discrepancies noted. Our energy levels are assessed to be accurate to better than 1% for a majority of levels, and A-values to better than 20% for most transitions. Collision strengths are also calculated, for which the Dirac Atomic R-matrix Code (DARC) is used. A wide energy range, up to 21 Ryd, is considered and resonances resolved in a fine energy mesh in the thresholds region. The collision strengths are subsequently averaged over a Maxwellian velocity distribution to determine effective collision strengths up to a temperature of 8.0×10^5 K, sufficient for most astrophysical applications. Our data are compared with the recent *R*-matrix calculations of Fernández-Menchero, Del Zanna & Badnell (2014), and significant differences (up to over an order of magnitude) are noted for several transitions over the complete temperature range of the results.

Key words: atomic data – atomic processes

1 INTRODUCTION

Observations of emission lines from Be-like ions, such as C III, O V, Ca XVII and Fe XXIII, provide useful diagnostics for density and temperature of astrophysical plasmas – see for example, Landi et al. (2001). Considering C III, early observations of strong emission (λ: 5696 Å) and absorption (λ: 4647 Å) features in HD 192639 were reported by Swings & Struve (1940). Keenan & Warren (1993) deduced electron densities using several line pairs arising from the $n = 2$ transitions of C III in solar spectra obtained by the Naval Research Laboratory's S082B instrument on board *Skylab*. More recently, strong emission lines of C III ($\lambda\lambda$ 4647-4650-4652 Å) have been detected in spectroscopic survey of Galactic O-type stars by Walborn et al. (2010). Similarly, among ultraviolet emission lines in young low-mass galaxies at redshift z $\sim$ 2, Stark et al. (2014) noted that the strongest (other than Lyα) is always the blended C III λ1908 doublet. Many observed lines of C III below 4700 Å are listed in the CHIANTI database at `http://www.chiantidatabase.org/`. Similarly, numerous transitions in the 270–2070 Å wavelength range are included in the *Atomic Line List* (v2.04) of Peter van Hoof at `http://www.pa.uky.edu/~peter/atomic/`.

For the reliable interpretation of observations, accurate atomic data are required for several parameters, such as energy levels, Einstein coefficients or radiative rates (A-values) and excitation rates – see section 6. Energy levels for C III have been calculated by several workers – see for example, Gu (2005) and references therein. Measurements of energy levels have been compiled and critically evaluated by the NIST (National Institute of Standards and Technology) team (Kramida et al. 2015) and are available at their website `http://www.nist.gov/pml/data/asd.cfm`. Similarly, A-values have been reported by numerous workers – see for example, Safronova et al. (1999a,b).

Since C III is an important ion in astrophysical (and fusion) plasmas, a few workers have reported data for collision strengths Ω, or more importantly *effective* collision strengths Υ, which are directly related to the excitation rates (section 6). Early *R*-matrix calculations were mostly performed by Berrington and his colleagues - see in particular Berrington et al. (1989) and references therein. These included 12 states among $n \leqslant 3$ configurations and were in *LS* coupling (Russell-Saunders or spin-orbit coupling). Subsequently, Mitnik et al. (2003) extended the calculations to

⋆ Tables 2, 7 and 8 are available only in the electronic version.

† E-mail: K.Aggarwal@qub.ac.uk(KMA); F.Keenan@qub.ac.uk (FPK)

24 states (including additional states of the $n = 4$ configurations), and made other improvements, particularly in the generation of wavefunctions. However, their results for Υ have been shown to be overestimated (by up to 50%, particularly at lower temperatures) for several important transitions, such as $2s^2\ ^1S_0 - 2s2p\ ^3P^o_{1,2}$ and $2s^2\ ^1S_0 - 2p^2\ ^1D_2$ – see fig. 3 of Fernández-Menchero, Del Zanna & Badnell (2014). The calculations of Fernández-Menchero et al. (2014) are not only the most recent but also the most extensive, because they have reported data for transitions among 238 *fine-structure* levels, belonging to the $n \leqslant 7$ configurations of C III.

To determine energy levels and A-values, Fernández-Menchero et al. (2014) adopted the *AutoStructure* (AS) code of Badnell (1997). The wave functions generated were subsequently employed in the *R*-matrix code of Berrington, Eissner & Norrington (1995) for the calculations of Ω, primarily obtained in *LS* coupling. Corresponding results for desired fine-structure transitions were determined through their intermediate coupling frame transformation (ICFT) method. Furthermore, they resolved resonances in the thresholds region to finally determine values of Υ. Since C III is a comparatively light ion, higher-order relativistic effects (neglected in the AS and *R*-matrix codes) are not very important, and hence their approach should give comparable results with a fully relativistic version, such as the Dirac atomic *R*-matrix code (DARC). Unfortunately, this is not the case as recently demonstrated by us (Aggarwal & Keenan 2015) for five other Be-like ions, namely Al X, Cl XIV, K XVI, Ti XIX and Ge XXIX. For about 50% of the transitions (of all ions) the Υ of Fernández-Menchero et al. (2014) are overestimated, up to more than an order of magnitude, and over a wide range of temperatures. Therefore, considering the importance of C III, we decided to perform yet another calculation so that atomic data can be confidently applied to the modelling of plasmas.

As in all our earlier work on Be-like ions, we have employed the fully relativistic GRASP (General-purpose Relativistic Atomic Structure Package) code, originally developed by Grant et al. (1980), but significantly revised by one of its authors (Dr. P. H. Norrington), and available at the website `http://web.am.qub.ac.uk/DARC/`, to determine the atomic structure, i.e. to calculate energy levels and A-values. Similarly for the scattering calculations, we have adopted the unpublished DARC code of P. H. Norrington and I. P. Grant, freely available at `http://web.am.qub.ac.uk/DARC/`). This is a relativistic version of the standard *R*-matrix code and is based on the *jj* coupling scheme.

2 ENERGY LEVELS

Our calculations for C III are larger than those performed by us for other Be-like ions. For this ion we have considered the energetically lowest 166 levels belonging to the 27 configurations: $(1s^2)\ 2\ell 2\ell'$, $2\ell 3\ell'$, $2\ell 4\ell'$ and $2\ell 5\ell'$, while for others (see Aggarwal & Keenan (2015) and references therein) the 68 levels of the $2\ell 5\ell'$ configurations were not considered. Our level energies calculated from GRASP, with the inclusion of Breit and QED (quantum electrodynamic) effects, are listed in Table 1 along with those of NIST and Fernández-Menchero et al. (2014).

Experimental energies are available for most of the levels, with a few exceptions such as 113–120. In Fig. 1 we show the differences (in percentage terms) between the experimental and theoretical energy levels. There is general agreement (within 1% for all levels) between our GRASP and the earlier AS energies of Fernández-Menchero et al. (2014), although our results are slightly closer to those of NIST. Differences between the theoretical and NIST energies are smaller than 1% for most levels. Unfortunately, the differences for the lowest 10 levels of the 2s2p and $2p^2$ configurations are significantly larger, up to 8%. Clearly there is scope for improvement which can (perhaps) be achieved by the inclusion of *pseudo* orbitals, as undertaken by Berrington et al. (1989) and Mitnik et al. (2003). This approach improves the accuracy of energy levels, although discrepancies with measurements remain up to 6% for a few, see for example the $2p^2\ ^1S_0$ level in table 1 of Mitnik et al. (2003). Therefore, there is little advantage in using pseudo orbitals, particularly because their inclusion gives rise to pseudo resonances in the subsequent scattering calculations for Ω. For this reason, neither ourselves nor Fernández-Menchero et al. (2014) have included pseudo orbitals in the generation of wavefunctions.

3 RADIATIVE RATES

We have calculated A-values for four types of transitions, namely electric dipole (E1), electric quadrupole (E2), magnetic dipole (M1) and magnetic quadrupole (M2) as all may be required in a plasma model (see e.g. Aggarwal & Keenan (2012) and references therein). The absorption oscillator strength (f_{ij}) and radiative rate A_{ji} (in s^{-1}) for all types of transition $i \rightarrow j$ are related by the following expression:

$$f_{ij} = \frac{mc}{8\pi^2 e^2}\lambda_{ji}^2 \frac{\omega_j}{\omega_i} A_{ji} = 1.49 \times 10^{-16} \lambda_{ji}^2 \frac{\omega_j}{\omega_i} A_{ji} \qquad (1)$$

where m and e are the electron mass and charge, respectively, c the velocity of light, λ_{ji} the transition energy/wavelength in Å, and ω_i and ω_j the statistical weights of the lower (i) and upper (j) levels, respectively. However, the relationships between oscillator strength f_{ij} (dimensionless) and the line strength S (in atomic unit, equivalent to 6.460×10^{-36} cm^2 esu^2) with the A-values differ for different types of transitions – see Eqs. (2–5) of Aggarwal & Keenan (2012).

Our calculated energies/wavelengths (λ, in Å), radiative rates (A_{ji}, in s^{-1}), oscillator strengths (f_{ij}, dimensionless), and line strengths (S, in atomic unit) are listed in Table 2 for all 3802 E1 transitions among the 166 levels of C III. The *indices* used to represent the lower and upper levels of a transition are defined in Table 1. Similarly, there are 4909 E2, 3728 M1 and 4975 M2 transitions among the same 166 levels. However, for these only the A-values are listed in Table 2. Corresponding data for f- values can be easily obtained through Eq. (1). Furthermore, results are only listed in the length form, which are considered to be comparatively more accurate. Nevertheless, below we discuss the velocity/length form ratio (R), as this provides some assessment of the accuracy of the data.

Table 1. Energy levels (in Ryd) of C III and their lifetimes (s). ($a\pm b \equiv a\times10^{\pm b}$).

Index	Configuration	Level	NIST	GRASP	AS	τ (s)
1	$2s^2$	$^1S_0$	0.00000	0.00000	0.00000	.....
2	2s2p	$^3P^o_0$	0.47720	0.48390	0.48949	.....
3	2s2p	$^3P^o_1$	0.47742	0.48409	0.48981	1.578−02
4	2s2p	$^3P^o_2$	0.47793	0.48457	0.49045	1.854+02
5	2s2p	$^1P^o_1$	0.93270	1.00439	1.00281	4.648−10
6	$2p^2$	$^3P_0$	1.25232	1.27817	1.29046	6.993−10
7	$2p^2$	$^3P_1$	1.25258	1.27842	1.29077	6.990−10
8	$2p^2$	$^3P_2$	1.25301	1.27880	1.29140	6.985−10
9	$2p^2$	$^1D_2$	1.32932	1.39544	1.40723	7.464−09
10	$2p^2$	$^1S_0$	1.66324	1.76957	1.77435	3.718−10
11	2s3s	$^3S_1$	2.17076	2.15962	2.14181	2.635−10
12	2s3s	$^1S_0$	2.25238	2.24672	2.23168	1.099−09
13	2s3p	$^3P^o_0$	2.36661	2.35629	2.34023	1.312−08
14	2s3p	$^3P^o_1$	2.36666	2.35632	2.34030	4.252−09
15	2s3p	$^3P^o_2$	2.36678	2.35646	2.34040	1.309−08
16	2s3p	$^1P^o_1$	2.35956	2.35674	2.33989	2.657−10
17	2s3d	$^3D_1$	2.46052	2.45212	2.43547	9.623−11
18	2s3d	$^3D_2$	2.46053	2.45213	2.43549	9.625−11
19	2s3d	$^3D_3$	2.46056	2.45215	2.43553	9.628−11
20	2s3d	$^1D_2$	2.51950	2.52902	2.50907	1.551−10
21	2p3s	$^3P^o_0$	2.80868	2.80571	2.79183	3.217−10
22	2p3s	$^3P^o_1$	2.80897	2.80600	2.79215	3.215−10
23	2p3s	$^3P^o_2$	2.80959	2.80660	2.79281	3.211−10
24	2s4s	$^3S_1$	2.81998	2.80756	2.79138	3.790−10
25	2p3s	$^1P^o_1$	2.82499	2.82522	2.81029	2.406−10
26	2s4s	$^1S_0$	2.84062	2.82683	2.81094	8.800−10
27	2s4p	$^3P^o_0$	2.89595	2.88219	2.86598	3.374−09
28	2s4p	$^3P^o_1$	2.89597	2.88220	2.86600	3.374−09
29	2s4p	$^3P^o_2$	2.89602	2.88225	2.86604	3.372−09
30	2p3p	$^1P_1$	2.91351	2.91034	2.89504	2.971−10
31	2s4d	$^3D_1$	2.92892	2.91830	2.90239	1.838−10
32	2s4d	$^3D_2$	2.92906	2.91836	2.90245	1.840−10
33	2s4d	$^3D_3$	2.92927	2.91846	2.90254	1.843−10
34	2s4f	$^3F^o_2$	2.93431	2.92159	2.90549	1.219−09
35	2s4f	$^3F^o_3$	2.93437	2.92163	2.90554	1.218−09
36	2s4f	$^3F^o_4$	2.93444	2.92169	2.90560	1.216−09
37	2s4f	$^1F^o_3$	2.94068	2.92696	2.91036	5.571−10
38	2p3p	$^3D_1$	2.94409	2.94399	2.92673	1.039−08
39	2p3p	$^3D_2$	2.94432	2.94428	2.92704	9.865−09
40	2p3p	$^3D_3$	2.94467	2.94475	2.92753	9.157−09
41	2s4d	$^1D_2$	2.95444	2.95066	2.93185	2.387−10
42	2s4p	$^1P^o_1$	2.93796	2.95239	2.93307	6.210−10
43	2p3p	$^3S_1$	2.98238	2.98492	2.96582	4.977−10
44	2p3p	$^3P_0$	3.00431	3.00370	2.99238	5.816−10
45	2p3p	$^3P_1$	3.00451	3.00388	2.99259	5.815−10
46	2p3p	$^3P_2$	3.00484	3.00419	2.99298	5.815−10
47	2p3d	$^1D^o_2$	3.03171	3.02604	3.01196	1.891−10
48	2p3d	$^3F^o_2$	3.03805	3.04299	3.02730	1.913−09
49	2p3d	$^3F^o_3$	3.03827	3.04322	3.02757	1.921−09
50	2p3d	$^3F^o_4$	3.03859	3.04355	3.02795	1.931−09

Ideally, R should be close to unity but often is not in (almost all) large calculations, such as the present one. As for other Be-like ions (Aggarwal & Keenan 2015), C III is no exception and hence the conclusions are similar. Specifically, for 453 strong E1 transitions ($f \geqslant 0.01$) R lies outside the range 0.8–1.2, i.e. is more than 20% away from unity. For most such transitions R is within a factor of two, but there are exceptions for a few, such as 5–121 (f = 0.05), 9–61 (f = 0.05), 19–145 (f = 0.01), 20–165 (f = 0.02) and 25–75 (f = 0.01). For these transitions unfortunately R is up to an order of magnitude. Similarly, for a few weaker transitions the two forms of f- values differ by up to several orders of magnitude, but most of these have very small f-values ($\sim10^{-5}$ or less). Nevertheless, such weak transitions may occasionally be important for the calculations of lifetimes, but should not significantly affect the modelling of plasmas.

Most of the A-values available in the literature involve levels of the $n \leqslant 3$ configurations. However, Fernández-Menchero et al. (2014) have reported results for a larger number of E1 transitions. For most there is satisfactory

Table 1. ... continued

Index	Configuration	Level	NIST	GRASP	AS	τ (s)
51	2p3p	$^1D_2$	3.03560	3.05501	3.04207	4.404−10
52	2p3d	$^3D^o_1$	3.07695	3.07184	3.05766	8.004−11
53	2p3d	$^3D^o_2$	3.07707	3.07195	3.05779	8.005−11
54	2p3d	$^3D^o_3$	3.07724	3.07212	3.05798	8.005−11
55	2s5s	$^1S_0$	3.08477	3.07632	3.06083	1.564−09
56	2s5s	$^3S_1$	3.09771	3.08391	3.06670	1.150−09
57	2p3d	$^3P^o_2$	3.09924	3.09682	3.08003	2.223−10
58	2p3d	$^3P^o_1$	3.09947	3.09699	3.08021	2.238−10
59	2p3d	$^3P^o_0$	3.09960	3.09708	3.08030	2.246−10
60	2s5f	$^1F^o_3$	3.11080	3.11518	3.09884	2.444−10
61	2s5p	$^1P^o_1$	3.12800	3.12205	3.10437	3.236−10
62	2s5p	$^3P^o_2$	3.13688	3.12668	3.10904	3.918−10
63	2s5p	$^3P^o_1$	3.13691	3.12677	3.10912	3.863−10
64	2s5p	$^3P^o_0$	3.13693	3.12683	3.10916	3.834−10
65	2s5d	$^3D_1$	3.14840	3.13429	3.11775	3.908−10
66	2s5d	$^3D_2$	3.14840	3.13430	3.11776	3.910−10
67	2s5d	$^3D_3$	3.14840	3.13430	3.11776	3.912−10
68	2s5g	$^3G_3$	3.15826	3.14245	3.12578	2.899−09
69	2s5g	$^3G_4$	3.15826	3.14245	3.12578	2.899−09
70	2s5g	$^3G_5$	3.15826	3.14245	3.12578	2.899−09
71	2s5g	$^1G_4$	3.15826	3.14246	3.12579	2.899−09
72	2s5f	$^3F^o_2$	3.16348	3.15099	3.13397	1.078−09
73	2s5f	$^3F^o_3$	3.16349	3.15101	3.13400	1.077−09
74	2s5f	$^3F^o_4$	3.16351	3.15105	3.13403	1.076−09
75	2s5d	$^1D_2$	3.15898	3.15210	3.13247	3.905−10
76	2p3d	$^1P^o_1$	3.15948	3.17556	3.15654	1.547−10
77	2p3p	$^1S_0$	3.14474	3.18667	3.15528	8.363−10
78	2p3d	$^1F^o_3$	3.17905	3.18957	3.17320	1.309−10
79	2p4s	$^3P^o_0$	3.42890	3.42158	3.40783	5.587−10
80	2p4s	$^3P^o_1$	3.42909	3.42188	3.40815	5.580−10
81	2p4s	$^3P^o_2$	3.43004	3.42250	3.40881	5.565−10
82	2p4s	$^1P^o_1$	3.47289	3.45238	3.44104	4.086−10
83	2p4p	$^1P_1$		3.46581	3.45272	3.562−10
84	2p4p	$^3D_1$	3.48058	3.47424	3.46093	8.093−10
85	2p4p	$^3D_2$	3.48078	3.47457	3.46127	8.105−10
86	2p4p	$^3D_3$	3.48113	3.47508	3.46180	8.103−10
87	2p4p	$^3S_1$		3.49002	3.47643	4.567−10
88	2p4p	$^3P_0$	3.50241	3.49717	3.48323	8.461−10
89	2p4p	$^3P_1$	3.50259	3.49736	3.48343	8.444−10
90	2p4p	$^3P_2$	3.50296	3.49766	3.48377	8.458−10
91	2p4d	$^1D^o_2$	3.51583	3.50794	3.49477	3.984−10
92	2p4d	$^3F^o_2$	3.51591	3.50991	3.49692	1.214−09
93	2p4d	$^3F^o_3$	3.51591	3.51017	3.49721	1.280−09
94	2p4d	$^3F^o_4$	3.51591	3.51060	3.49767	1.283−09
95	2p4p	$^1D_2$	3.51419	3.51943	3.50408	5.997−10
96	2p4d	$^3D^o_1$	3.53296	3.52476	3.51043	1.661−10
97	2p4d	$^3D^o_2$	3.53296	3.52487	3.51055	1.662−10
98	2p4d	$^3D^o_3$	3.53296	3.52504	3.51074	1.661−10
99	2p4f	$^1F_3$	3.54276	3.52790	3.51381	6.067−10
100	2p4f	$^3F_2$	3.53728	3.52842	3.51444	6.357−10

agreement between the two calculations, but for a few weak(er) ones there are discrepancies of over 50%, as shown in Table 3. Such discrepancies between any two calculations often arise for weak(er) transitions, mainly due to the different levels of CI included and/or the method adopted. The A-values for a few M1 transitions are also available in the literature, mainly by Glass (1983) and Safronova et al. (1999b). In Table 4 we compare our A-values for the common transitions. As expected, all such transitions are weak and there is generally no large discrepancy. However, for the 3–5 transition there is a significant differences in the A-values, as our result is larger than of Safronova et al. (1999b) by a factor of two, but is lower than of Glass (1983) by a factor of four. However, Nussbaumer & Storey (1978) calculated an A-value of 1.09×10^{-3} s^{-1} for this transition, which agrees within 20% with our result.

4 LIFETIMES

The lifetime τ for a level j is defined as follows:

Table 1. ... continued

Index	Configuration	Level	NIST	GRASP	AS	τ (s)
101	2p4f	$^3F_3$	3.53739	3.52851	3.51453	6.351−10
102	2p4f	$^3F_4$	3.53767	3.52860	3.51464	6.357−10
103	2p4d	$^3P^o_2$	3.54021	3.53408	3.51984	2.603−10
104	2p4d	$^3P^o_1$	3.54021	3.53437	3.52013	2.600−10
105	2p4d	$^3P^o_0$	3.54021	3.53452	3.52028	2.599−10
106	2p4f	$^3G_3$	3.53686	3.53684	3.52268	7.018−10
107	2p4f	$^3G_4$	3.53686	3.53711	3.52297	7.037−10
108	2p4f	$^3G_5$	3.53686	3.53754	3.52341	7.016−10
109	2p4f	$^1G_4$		3.54008	3.52645	8.822−10
110	2p4f	$^3D_3$	3.55092	3.54326	3.52920	6.765−10
111	2p4f	$^3D_2$	3.55140	3.54355	3.52950	6.764−10
112	2p4f	$^3D_1$	3.55153	3.54378	3.52973	6.761−10
113	2p4f	$^1D_2$		3.54683	3.53305	7.084−10
114	2p4d	$^1F^o_3$		3.56068	3.54287	1.394−10
115	2p4d	$^1P^o_1$		3.56868	3.55002	2.266−10
116	2p4p	$^1S_0$		3.57681	3.55737	1.482−09
117	2p5s	$^3P^o_0$		3.68170	3.66788	7.601−10
118	2p5s	$^3P^o_1$		3.68200	3.66819	7.576−10
119	2p5s	$^3P^o_2$		3.68263	3.66886	7.550−10
120	2p5s	$^1P^o_1$		3.69465	3.68074	3.997−10
121	2p5p	$^1P_1$	3.71278	3.70468	3.69117	2.670−10
122	2p5p	$^3D_1$	3.71638	3.70779	3.69433	7.797−10
123	2p5p	$^3D_2$	3.71638	3.70808	3.69463	7.938−10
124	2p5p	$^3D_3$	3.71638	3.70858	3.69515	7.934−10
125	2p5p	$^3S_1$		3.71476	3.70116	3.248−10
126	2p5p	$^3P_0$	3.72640	3.71875	3.70457	1.084−09
127	2p5p	$^3P_1$	3.72640	3.71895	3.70479	1.066−09
128	2p5p	$^3P_2$	3.72640	3.71923	3.70510	1.083−09
129	2p5d	$^1D^o_2$	3.73331	3.72472	3.71123	7.188−10
130	2p5d	$^3F^o_2$		3.72544	3.71206	1.237−09
131	2p5d	$^3F^o_3$		3.72558	3.71223	1.786−09
132	2p5d	$^3F^o_4$		3.72602	3.71270	1.809−09
133	2p5p	$^1D_2$	3.73169	3.73175	3.71533	5.258−10
134	2p5d	$^3D^o_1$	3.74153	3.73248	3.71838	2.344−10
135	2p5d	$^3D^o_2$	3.74153	3.73259	3.71850	2.350−10
136	2p5d	$^3D^o_3$	3.74153	3.73278	3.71870	2.345−10
137	2p5f	$^1F_3$		3.73419	3.72026	1.024−09
138	2p5f	$^3F_2$	3.74406	3.73453	3.72064	1.043−09
139	2p5f	$^3F_3$	3.74406	3.73461	3.72072	1.048−09
140	2p5f	$^3F_4$	3.74406	3.73469	3.72082	1.050−09
141	2p5g	$^3G^o_4$	3.74626	3.73626	3.72235	1.469−09
142	2p5g	$^3G^o_3$	3.74626	3.73626	3.72236	1.470−09
143	2p5g	$^1G^o_4$	3.74626	3.73638	3.72247	1.487−09
144	2p5g	$^3G^o_5$		3.73638	3.72248	1.488−09
145	2p5d	$^3P^o_2$	3.74432	3.73645	3.72224	3.287−10
146	2p5d	$^3P^o_1$	3.74432	3.73673	3.72252	3.284−10
147	2p5d	$^3P^o_0$	3.74432	3.73687	3.72267	3.286−10
148	2p5f	$^3G_3$	3.74366	3.73773	3.72370	1.269−09
149	2p5f	$^3G_4$	3.74366	3.73798	3.72396	1.275−09
150	2p5g	$^3H^o_4$	3.74585	3.73846	3.72461	1.967−09

$$\tau_j = \frac{1}{\sum_i A_{ji}}. \quad (2)$$

Since this is a measurable quantity, it facilitates an assessment of the accuracy of the A-values, particularly when a single transition dominates the contributions. Therefore, in Table 1 we have also listed our calculated lifetimes. Generally, A-values for E1 transitions are considerably larger in magnitude and hence dominate the determination of τ, but for higher accuracy we have also included the contributions from E2, M1 and M2. Their inclusion is particularly important for those levels for which either E1 transitions do not exist or are dominated by others.

There have been several measurements of τ for a few levels of C III, and results up to 1990 have been compiled by Allard et al. (1990). In Table 5 we compare our data with their compilation. For some levels there are several measurements and therefore we have listed the *range* for convenience (specific results are given in table IIIa of Allard et al. (1990)). Most levels show reasonable agreement (within a few percent) between theory and measurement. However,

Table 1. ... continued

Index	Configuration	Level	NIST	GRASP	AS	τ (s)
151	2p5g	$^3H^o_5$	3.74585	3.73848	3.72464	1.974−09
152	2p5f	$^3G_5$	3.74366	3.73839	3.72439	1.272−09
153	2p5g	$^3H^o_6$	3.74585	3.73907	3.72525	1.995−09
154	2p5g	$^1H^o_5$		3.73910	3.72529	2.004−09
155	2p5g	$^3F^o_4$	3.74925	3.73986	3.72604	1.364−09
156	2p5g	$^1F^o_3$		3.73988	3.72607	1.367−09
157	2p5f	$^1G_4$		3.74023	3.72646	1.525−09
158	2p5g	$^3F^o_2$	3.74925	3.74036	3.72656	1.360−09
159	2p5g	$^3F^o_3$	3.74925	3.74037	3.72658	1.362−09
160	2p5f	$^3D_3$		3.74175	3.72769	8.861−10
161	2p5f	$^3D_2$		3.74203	3.72798	8.823−10
162	2p5f	$^3D_1$		3.74225	3.72821	8.842−10
163	2p5f	$^1D_2$		3.74516	3.73082	6.213−10
164	2p5d	$^1F^o_3$		3.75389	3.73497	1.342−10
165	2p5d	$^1P^o_1$		3.76002	3.73894	1.739−10
166	2p5p	$^1S_0$		3.78461	3.74510	7.954−10

NIST: `http://www.nist.gov/pml/data/asd.cfm`
GRASP: Energies from the GRASP code for 166 level calculations
AS: Energies from the AS for 238 level calculations

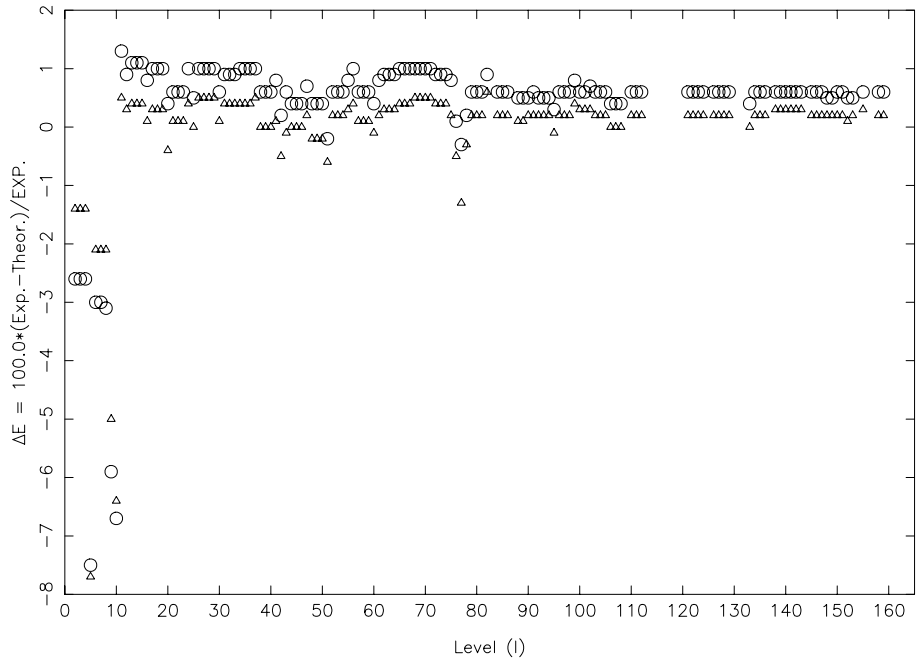

Figure 1. Percentage differences between experimental and theoretical energy levels. Triangles: present calculations with GRASP and circles: calculations of Fernández-Menchero et al. (2014) with AS.

there are also striking discrepancies for five, namely 2p3p ^{1}P, 2p3p ^{3}S, 2p3d $^1P^o$, 2s5f ^{1}D and 2p5g $^3G^o$, where the only available measurements are from Poulizac & Buchet (1971) and Poulizac, Druetta & Ceyseriat (1971). For the 2p3d $^1P^o$ level the discrepancy is the largest (by a factor of 50), but our result of 0.155 ns agrees closely with the calculations of Allard et al. (1990), i.e. 0.17 ns. Similarly, for other levels where there are large discrepancies in Table 5 there is satisfactory agreement between our results and the calculations of Allard et al. (1990). Therefore, for the 2p3d $^1P^o$ level the measured τ of Poulizac et al. (1971) appears to be incorrect. Nandi et al. (1996) have measured τ for 2p^2 ^{1}D and 2s3p $^3P^o$ to be 6.9±0.2 and 11.6±0.3 ns, respectively and for both there is no large discrepancy with our calculations (7.5 and 13.1 ns, respectively) or other earlier experimental values.

Tachiev & Froese Fischer (1999) have calculated τ for the lowest 20 levels of C III and their results are compared

Table 2. Transition wavelengths (λ_{ij} in Å), radiative rates (A_{ji} in s^{-1}), oscillator strengths (f_{ij}, dimensionless), and line strengths (S, in atomic units) for electric dipole (E1), and A_{ji} for E2, M1 and M2 transitions in C III. ($a\pm b \equiv a\times10^{\pm b}$). See Table 1 for level indices.

i	j	λ_{ij}	A_{ji}^{E1}	f_{ij}^{E1}	S^{E1}	A_{ji}^{E2}	A_{ji}^{M1}	A_{ji}^{M2}
1	3	1.882+03	6.338+01	1.010−07	6.260−07	0.000+00	0.000+00	0.000+00
1	4	1.881+03	0.000+00	0.000+00	0.000+00	0.000+00	0.000+00	5.390−03
1	5	9.073+02	2.152+09	7.966−01	2.379+00	0.000+00	0.000+00	0.000+00
1	7	7.128+02	0.000+00	0.000+00	0.000+00	0.000+00	8.478−04	0.000+00
1	8	7.126+02	0.000+00	0.000+00	0.000+00	1.953−02	0.000+00	0.000+00
1	9	6.530+02	0.000+00	0.000+00	0.000+00	3.605+03	0.000+00	0.000+00
...								
...								
...								

Table 3. Comparison of A-values for a few E1 transitions of C III. ($a\pm b \equiv a\times10^{\pm b}$). See Table 1 for level indices.

I	J	f (GRASP)	A (GRASP)	A (AS)	R
1	3	1.010−07	6.338+01	1.120+02	1.8
1	28	8.452−09	1.880+02	4.870+02	2.6
1	61	7.696−02	2.009+09	1.280+09	1.6
1	63	2.386−06	6.245+04	3.300+04	1.9
1	76	2.064−04	5.573+06	7.930+07	14.2
2	38	4.312−04	6.988+06	1.610+07	2.3
3	9	3.412−07	1.366+03	2.260+03	1.7
3	10	2.872−08	1.144+03	1.750+03	1.5
3	12	4.814−09	3.604+02	2.230+02	1.6
3	20	5.632−08	1.135+03	2.390+03	2.1
3	26	3.621−11	4.789+00	3.000+02	62.6
3	38	1.009−04	4.906+06	1.150+07	2.3
3	39	3.911−04	1.141+07	2.470+07	2.2
3	75	5.931−08	2.035+03	8.050+02	2.5
3	77	1.780−08	3.132+03	5.880+03	1.9
4	9	2.272−06	1.514+04	2.310+04	1.5
4	20	9.300−10	3.122+01	1.980+01	1.6
4	38	3.531−06	2.860+05	7.040+05	2.5
4	39	6.941−05	3.373+06	7.550+06	2.2
4	40	5.495−04	1.908+07	3.850+07	2.0
4	68	4.182−13	1.695−02	4.130−02	2.4
5	6	5.620−08	1.015+02	2.120+02	2.1
5	7	6.737−09	4.064+00	8.780+00	2.2
5	8	8.681−07	3.150+02	5.670+02	1.8
5	11	4.830−08	5.178+02	9.030+02	1.7
5	17	6.667−08	1.122+03	1.750+03	1.6
5	18	6.090−08	6.152+02	1.690+03	2.7
5	24	8.707−09	2.274+02	4.170+00	54.5
5	32	1.532−07	2.706+03	1.190+03	2.3
5	46	1.813−06	3.495+04	5.660+04	1.6
5	56	1.935−09	6.722+01	2.260+01	3.0
5	65	4.203−09	1.531+02	3.870+02	2.5
5	66	5.046−10	1.103+01	2.270+02	20.6
5	75	9.435−02	2.097+09	1.160+09	1.8
5	77	8.216−03	9.429+08	2.600+08	3.6

GRASP: Present calculations with the GRASP code
AS: Calculations of Fernández-Menchero et al. (2014) with the AS code
R: ratio of GRASP and AS A-values, the larger of the two is always in the nemerator

with ours in Table 6. The only level for which there is a serious discrepancy is 2s3p $^3P_1^o$, with our value lower by about a factor of three. This is because in our calculations the A(f)-value for the $2s^2\ ^1S_0$–$3s3p\ ^3P_1^o$ transition is 1.362×10^8 s^{-1} (9.16×10^{-3}) while theirs is 5.18×10^5 s^{-1} (3.45×10^{-5}). However, being intercombination it is a weak transition and therefore its A(f) values fluctuate with differing amount of CI and methods. For example, the A-value reported by Safronova et al. (1999a) is 8.41×10^4 s^{-1} whereas Cheng & Chen (2008) calculated A = 1.0×10^2 s^{-1}. Therefore, due to

Table 4. Comparison of A-values for a few M1 transitions of C III. ($a\pm b \equiv a\times10^{\pm b}$). See Table 1 for level indices.

I	J	Present	Glass (1983)	Safronova et al. (1999b)
1	7	8.478−4	5.335−4	6.53−4
2	3	1.697−7	2.162−7	2.68−7
2	5	1.480−3	1.592−3	6.12−3
3	4	1.948−6	2.139−6	2.50−6
3	5	1.293−3	5.676−3	5.52−4
4	5	1.943−3	1.981−3	8.28−4
6	7	3.483−7	4.092−7	4.52−7
7	8	9.745−7	1.316−6	1.73−6
7	9	2.455−4	1.982−4	1.16−5
7	10	1.483−2	1.924−2	4.68−3
8	9	7.578−4	6.296−4	3.64−5

Table 5. Comparison of lifetimes (τ, ns) for a few levels of C III.

Configuration/Level	Present	Allard et al. (1990)
2s2p ^{1}P^o	0.465	0.50–0.66
2p^2 ^{3}P	0.700	0.74–0.90
2p^2 ^{1}D	7.464	6.90–9.30
2p^2 ^{1}S	0.372	0.39–0.58
2s3s ^{3}S	0.264	0.32–0.37
2s3s ^{1}S	1.099	0.61–1.25
2s3p ^{1}P^o	0.266	0.255–0.370
2s3p ^{3}P^o	13.100	12.5–15.1
2s3d ^{3}D	0.096	0.115–0.120
2s3d ^{1}D	0.155	0.14–0.30
2p3s ^{3}P^o	0.322	0.374–0.400
2p3s ^{1}P^o	0.241	0.26–0.93
2p3p ^{1}P	0.297	0.59
2p3p ^{3}S	0.498	2.3
2p3p ^{3}P	0.582	0.45–0.70
2p3p ^{1}D	0.440	0.38–0.53
2p3p ^{1}S	0.836	1.3
2p3d ^{3}F^o	1.921	2.3
2p3d ^{3}D^o	0.080	0.088–0.100
2p3d ^{1}D^o	0.189	0.140–0.191
2p3d ^{3}P^o	0.224	0.179–2.500
2p3d ^{1}F^o	0.131	0.120–0.124
2p3d ^{1}P^o	0.155	7.8
2s4s ^{3}S	0.379	0.45–0.56
2s4p ^{1}P^o	0.621	0.56–0.60
2s4d ^{3}D	0.184	0.175–2.900
2s4d ^{1}D	0.239	0.35–0.36
2s4f ^{3}F^o	1.218	1.5–1.6
2s4f ^{1}F^o	0.557	0.32–1.00
2s5s ^{3}S	1.150	1.3
2s5p ^{3}P^o	0.390	0.33–0.90
2s5d ^{3}D	0.391	0.50
2s5d ^{1}D	0.391	0.82
2s5f ^{3}F^o	1.077	1.0-1.2
2s5f ^{1}F^o	0.244	0.3
2s5g ^{3}G	2.899	3.3
2s5g ^{1}G	2.899	3.6
2p5g ^{3}G^o	1.470	0.7

Table 6. Comparison of lifetimes (τ, s) for the lowest 20 levels of C III. ($a\pm b \equiv a\times10^{\pm b}$).

Index	Configuration	Level	Present	Tachiev & Froese Fischer (1999)
1	$2s^2$	$^1S_0$	.....	.....
2	2s2p	$^3P^o_0$	.....	.....
3	2s2p	$^3P^o_1$	1.578−02	9.616−03
4	2s2p	$^3P^o_2$	1.854+02	1.916+02
5	2s2p	$^1P^o_1$	4.648−10	5.615−10
6	$2p^2$	$^3P_0$	6.993−10	7.571−10
7	$2p^2$	$^3P_1$	6.990−10	7.567−10
8	$2p^2$	$^3P_2$	6.985−10	7.562−10
9	$2p^2$	$^1D_2$	7.464−09	7.191−09
10	$2p^2$	$^1S_0$	3.718−10	4.764−10
11	2s3s	$^3S_1$	2.635−10	2.709−10
12	2s3s	$^1S_0$	1.099−09	1.171−09
13	2s3p	$^3P^o_0$	1.312−08	1.352−08
14	2s3p	$^3P^o_1$	4.252−09	1.340−08
15	2s3p	$^3P^o_2$	1.309−08	1.347−08
16	2s3p	$^1P^o_1$	2.657−10	2.512−10
17	2s3d	$^3D_1$	9.623−11	9.400−11
18	2s3d	$^3D_2$	9.625−11	9.402−11
19	2s3d	$^3D_3$	9.628−11	9.404−11
20	2s3d	$^1D_2$	1.551−10	1.589−10

Table 7. Collision strengths for resonance transitions of C III. ($a\pm b \equiv a\times10^{\pm b}$). See Table 1 for level indices.

Transition		Energy (Ryd)			
i	j	5	10	15	20
1	2	2.691−02	1.153−02	5.983−03	3.613−03
1	3	8.073−02	3.460−02	1.795−02	1.084−02
1	4	1.345−01	5.763−02	2.990−02	1.805−02
1	5	7.240+00	9.860+00	1.144+01	1.260+01
1	6	5.215−04	1.890−04	8.446−05	4.416−05
1	7	1.563−03	5.661−04	2.524−04	1.317−04
1	8	2.607−03	9.456−04	4.232−04	2.221−04
1	9	2.938−01	2.760−01	2.646−01	2.585−01
1	10	7.496−02	7.864−02	7.479−02	7.049−02
...					
...					
...					

the paucity of measurements for this level, it is difficult to fully assess the accuracy of any calculation. Nevertheless, since there is a general agreement between theory and measurement for most of the levels/states as shown in Tables 5 and 6, we are confident that our calculations for A, f and τ are accurate to better than 20% for a majority of transitions (levels).

5 COLLISION STRENGTHS

The collision strength for electron impact excitation (Ω) is a symmetric and dimensionless quantity, related to the better-known parameter collision cross section (σ_{ij}) – see eq. (7) of Aggarwal & Keenan (2012). As stated earlier and in our work on other Be-like ions, we have adopted the relativistic DARC code for calculating Ω. It is based on the jj coupling scheme and uses the Dirac-Coulomb Hamiltonian in an R-matrix approach. The R-matrix radius adopted for C III is 28.0 atomic unit, and 55 continuum orbitals have been included for each channel angular momentum in the expansion of the wavefunction. This large expansion has become necessary to compute Ω up to an energy of 21 Ryd, so that the subsequent values of effective collision strength Υ (see section 6) can be reliably calculated up to $T_e = 8.0\times10^5$ K, well above the temperature of maximum abundance in ionisation equilibrium for C III, i.e. 7.9 $\times10^4$ K (Bryans, Landi & Savin 2009). However, considering the number of levels involved (166) the maximum number of channels generated for a partial wave is 828, and the corresponding size of the Hamiltonian (H) matrix becomes 45 714. Therefore, the present calculations are computationally more demanding and challenging than for other Be-like ions, such as Ti XIX (Aggarwal & Keenan 2012) for which the size of H was only 23 579. Furthermore, to achieve convergence of Ω for a majority of transitions and at all energies, we have included all

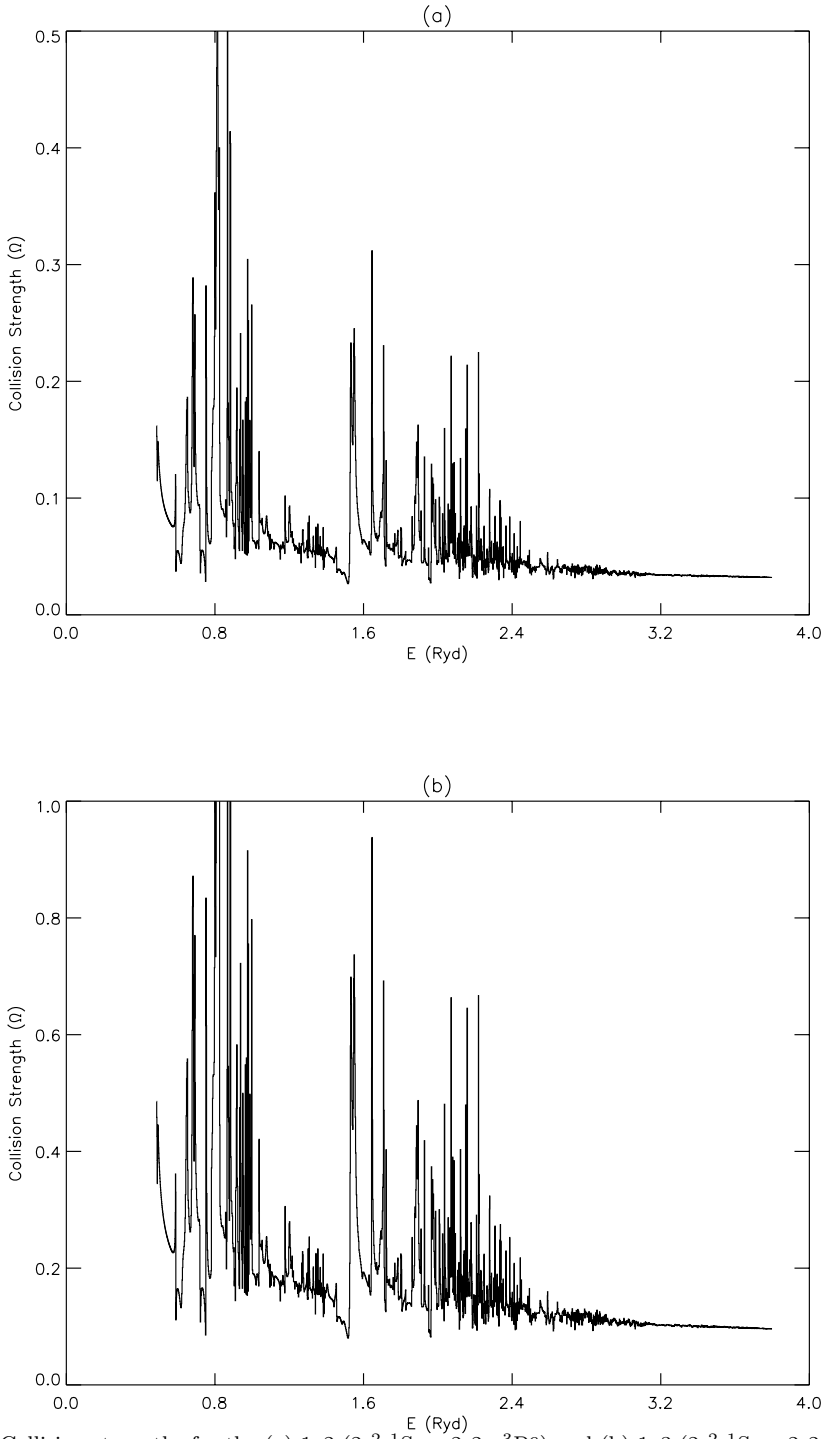

Figure 2. Collision strengths for the (a) 1–2 ($2s^2\ ^1S_0 - 2s2p\ ^3P^o_0$) and (b) 1–3 ($2s^2\ ^1S_0 - 2s2p\ ^3P^o_1$) transition of C III.

partial waves with angular momentum $J \leqslant 40.5$. To account for higher neglected partial waves we have included a top-up in the same way as for other ions, i.e. the Coulomb-Bethe (Burgess & Sheorey 1974) and geometric series approximations for allowed and forbidden transitions, respectively. For most transitions and at most energies these contributions are small but nevertheless make our calculated values of Ω comparatively more accurate.

No theoretical or experimental data for Ω are available for comparison with our results. However, in Table 7 we list our values of Ω for resonance transitions of C III at four energies *above* thresholds, i.e. 5, 10, 15 and 20 Ryd. The in-

dices used to represent the levels of a transition have already been defined in Table 1. We hope our results in the table for Ω will be useful for future comparison with experimental and other theoretical data. In the threshold energy region, Ω does not vary smoothly, especially for (semi) forbidden transitions. There often are numerous closed-channel (Feshbach) resonances in this region, as shown in fig. 2 of Fernández-Menchero et al. (2014) for four transitions, namely 1–3 ($2s^2\ ^1S_0$ – $2s2p\ ^3P^o_1$), 1–4 ($2s^2\ ^1S_0$ – $2s2p\ ^3P^o_2$), 1–5 ($2s^2\ ^1S_0$ – $2s2p\ ^1P^o_1$) and 1–9 ($2s^2\ ^1S_0$ – $2p^2\ ^1D_2$). We observe similar resonances, in both frequency and magnitude, and for illustration show these in Fig. 2 (a and b) for two transitions, i.e. 1–2 ($2s^2\ ^1S_0$ – $2s2p\ ^3P^o_0$) and 1–3 ($2s^2\ ^1S_0$ – $2s2p\ ^3P^o_1$). The first is a forbidden transition whereas the second is inter-combination.

6 EFFECTIVE COLLISION STRENGTHS

Since Ω does not vary smoothly with energy, as shown in Fig. 2, it is the *effective* collision strength (Υ) which is required in plasma modelling applications. This is determined from the collision strengths (Ω) by averaging over a suitable distribution of electron velocities. The most appropriate and widely used distribution for applications in astrophysics is *Maxwellian* and hence is adopted in both earlier and the present work, and also by Fernández-Menchero et al. (2014). The presence of resonances is generally significant for forbidden, semi-forbidden and inter-combination transitions (see Fig. 2) and therefore for these the enhancement in the values of Υ is substantial. Similarly, values of Υ are affected more towards the lower range of temperatures. Such enhancements have already been noted for a wide range of ions, including Be-like (Aggarwal & Keenan 2015). However, to account for their contribution resonances need to be resolved in a fine energy mesh. Fortunately, resonances for transitions in C III are not very dense, as may be seen from our Fig. 2 and fig. 2 of Fernández-Menchero et al. (2014). Nevertheless, we have performed our calculations of Ω at ∼2500 energies in the thresholds region with a mesh of (generally) 0.001 Ryd to calculate Υ, which is given by:

$$\Upsilon(T_e) = \int_0^\infty \Omega(E) \exp(-E_j/kT_e)\, d(E_j/kT_e), \qquad (3)$$

where k is Boltzmann constant, T_e the electron temperature in K, and E_j the electron energy with respect to the final (excited) state. Once the value of Υ is known the corresponding results for the excitation q(i,j) and de-excitation q(j,i) rates can be easily obtained from the following equations:

$$q(i,j) = \frac{8.63 \times 10^{-6}}{\omega_i T_e^{1/2}} \Upsilon \exp(-E_{ij}/kT_e) \qquad \mathrm{cm^3 s^{-1}} \qquad (4)$$

and

$$q(j,i) = \frac{8.63 \times 10^{-6}}{\omega_j T_e^{1/2}} \Upsilon \qquad \mathrm{cm^3 s^{-1}}, \qquad (5)$$

where ω_i and ω_j are the statistical weights of the initial (i) and final (j) states, respectively, and E_{ij} is the transition energy.

Our calculated values of Υ are listed in Table 8 over a wide temperature range up to $10^{5.9}$ K, suitable for applications to a wide range of astrophysical (and laboratory) plasmas. Corresponding data at any intermediate temperature can be easily interpolated, because (unlike Ω) Υ is a slowly varying function of T_e. As already noted in section 1, the most recent, extensive and perhaps best available corresponding data for Υ are those by Fernández-Menchero et al. (2014). Similar to ourselves, they have adopted the (semi-relativistic) *R*-matrix code, resolved resonances in a fine energy mesh, averaged Ω over a Maxwellian distribution, and reported results for transitions among 238 levels, over a wide range of electron temperature up to $1.8{\times}10^7$ K. Therefore, we undertake a comparison only with their results.

In Table 9 we compare our results for Υ with those of Fernández-Menchero et al. (2014) at three temperatures of 1800, 90 000 and 450 000 K, for resonance transitions up to level 78. The first and the third are the lowest and the highest *common* temperatures between the two calculations whereas the second is the most appropriate for applications to astrophysical plasmas, as already mentioned in section 5. Comparisons of Υ for all transitions among the lowest 78 levels at these three temperatures are shown in Fig. 3 (a, b and c) in the form of the ratio $R = \Upsilon_{DARC}/\Upsilon_{ICFT}$. Note that negative values of R represent $\Upsilon_{ICFT}/\Upsilon_{DARC}$, i.e. $\Upsilon_{ICFT} > \Upsilon_{DARC}$. At the two higher values of T_e, the two sets of Υ generally agree within 20% for most of the transitions listed in Table 9. However, differences are larger (up to a factor of two) for a few, particularly those with upper levels > 60. Unfortunately, the discrepancies are larger (up to a factor of two) at the lowest temperature of 1800 K, for about half the transitions, and in a majority of cases $\Upsilon_{ICFT} > \Upsilon_{DARC}$. Such discrepancies at low temperatures are not uncommon and mostly arise due to the position of resonances, because 1800 K is equivalent to only ∼0.011 Ryd, whereas our adopted energy mesh is 0.001 Ryd. To reliably calculate Υ at such low temperature(s), the energy mesh needs to be *finer* because our tests show that the uncertainty introduced by our (comparatively) coarse mesh is ∼20% at T_e = 1800 K.

Fernández-Menchero et al. (2014) adopted a comparatively finer energy mesh of 0.000 04 Ryd, but only for $J \leqslant 11.5$ for which they performed the *electron-exchange* calculations. For higher partial waves, up to $J = 45$, they adopted a coarser mesh of 0.004 Ryd in a *no-exchange* calculation. These two different meshes should not normally matter for calculations of Υ at low temperatures, such as 1800 K, because $J \leqslant 11.5$ should be sufficient for the convergence of Ω at low energies. Therefore, their reported Υ *may be* comparatively more accurate at this T_e. For transitions among all levels, in most cases the Υ of Fernández-Menchero et al. (2014) are larger as shown in Fig. 3a, but in a few instances $\Upsilon_{DARC} > \Upsilon_{ICFT}$. Examples where our data are larger include transitions 38–56, 39–56 and 40–56, which are *forbidden* and have resonances close to the thresholds. As the calculations of Fernández-Menchero et al. (2014) are primarily in *LS* coupling, there is a possibility of these resonances being missed. Nevertheless, this low temperature of 1800 K is not generally expected to be important for applications in plasma modelling and therefore we focus our attention on comparison at the two higher temperatures.

As shown in Fig. 3 (b and c) the discrepancies between our calculations and those of Fernández-Menchero et al. (2014) increase with increasing temperature. For about one fifth of the transitions, the differences are larger than

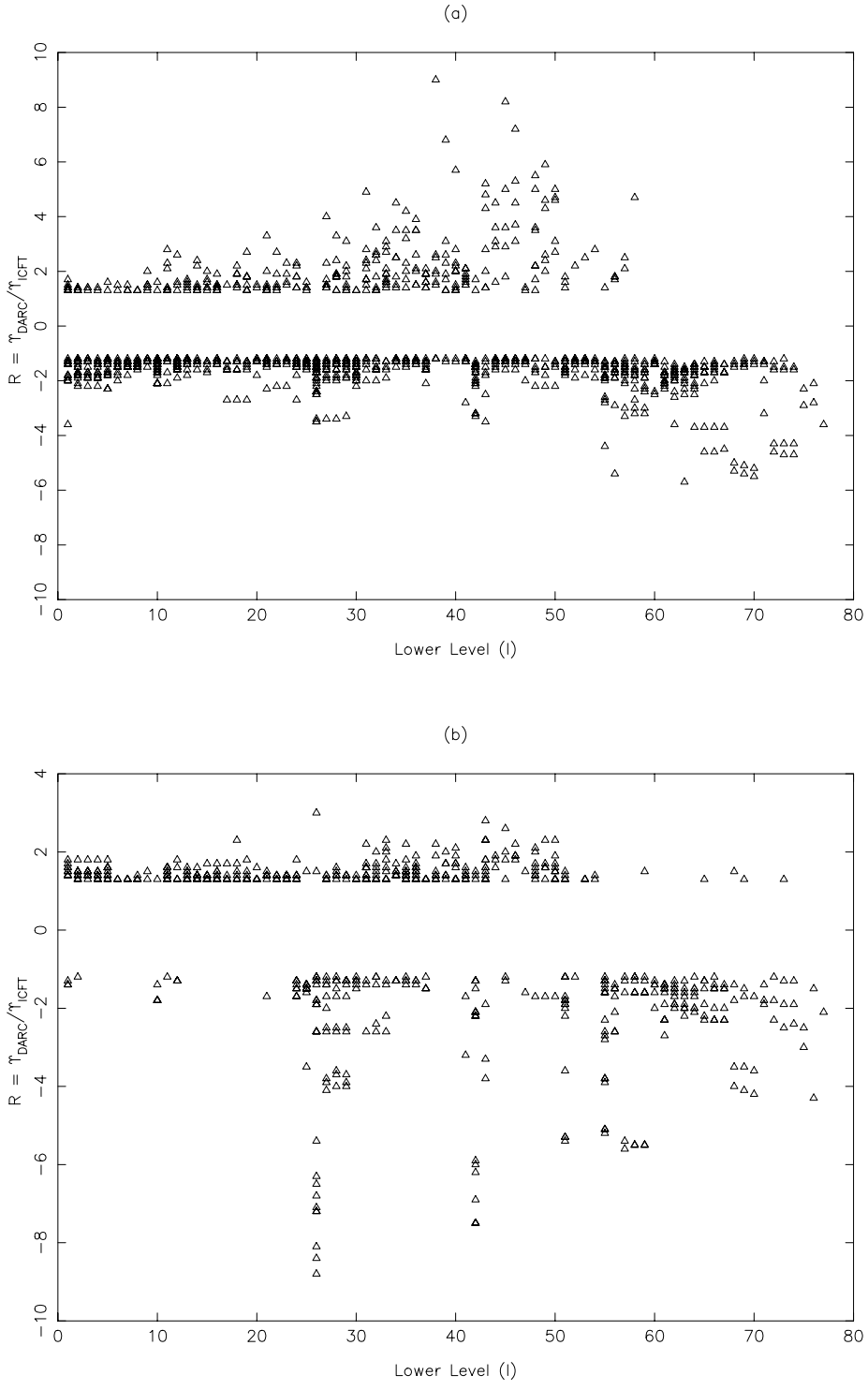

20%, and in a majority of cases $\Upsilon_{ICFT} > \Upsilon_{DARC}$, by up to a factor of 20. These discrepancies between the two independent calculations are consistent with those already found for other Be-like ions, namely Al X, Cl XIV, K XVI, Ti XIX and Ge XXIX (Aggarwal & Keenan 2015). As discussed in Aggarwal & Keenan (2015), the main source of inaccuracy in the calculations of Fernández-Menchero et al. (2014) for Υ is the use of a limited energy range for calculating Ω, up to only 11 Ryd which is insufficient for the determination of Υ up to 1.8×10^7 K (or equivalently to 114 Ryd), because the integral in Eq. (3) will not converge, although they have extended the energy range of Ω following the suggested formulae of Burgess & Tully (1992). However, in our work there is no requirement for such an extension because calculations for Ω have already been performed up to sufficiently high energies, as detailed in section 5. Therefore, based on the comparisons discussed here as well as for other Be-like ions and shown in Fig. 3, the results of Υ by Fernández-Menchero

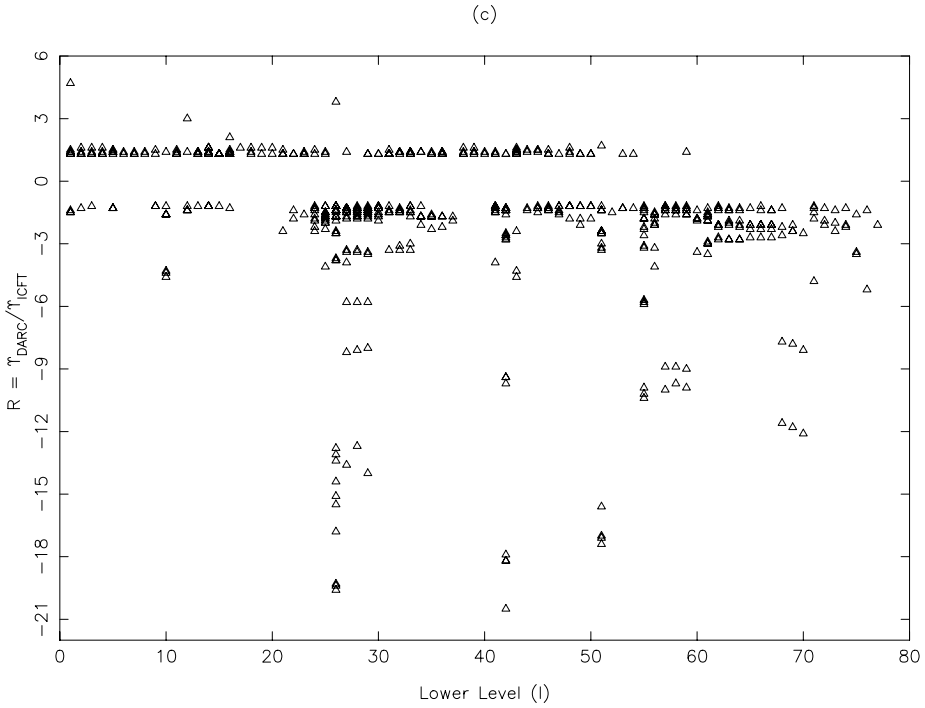

Figure 3. Comparison of DARC and ICFT Υ for transitions of C III at (a) T_e = 1800 K, (b) T_e = 90 000 K and (c) T_e = 450 000 K. Negative R values indicate that $\Upsilon_{\rm ICFT} > \Upsilon_{\rm DARC}$.

Table 8. Effective collision strengths for transitions in C III. ($a\pm b \equiv a\times10^{\pm b}$). See Table 1 for level indices.

Transition		Temperature (log T_e, K)							
i	j	4.50	4.70	4.90	5.10	5.30	5.50	5.70	5.90
1	2	1.042−01	1.028−01	9.681−02	8.742−02	7.608−02	6.402−02	5.216−02	4.107−02
1	3	3.132−01	3.090−01	2.907−01	2.625−01	2.284−01	1.922−01	1.566−01	1.233−01
1	4	5.238−01	5.161−01	4.853−01	4.380−01	3.810−01	3.206−01	2.612−01	2.056−01
1	5	3.588+00	3.742+00	3.961+00	4.274+00	4.720+00	5.337+00	6.124+00	6.901+00
1	6	3.144−03	3.041−03	2.852−03	2.546−03	2.152−03	1.733−03	1.341−03	1.002−03
1	7	9.452−03	9.132−03	8.558−03	7.633−03	6.449−03	5.193−03	4.017−03	3.001−03
1	8	1.583−02	1.528−02	1.432−02	1.277−02	1.079−02	8.684−03	6.717−03	5.017−03
1	9	3.409−01	3.476−01	3.477−01	3.413−01	3.314−01	3.205−01	3.094−01	2.945−01
1	10	8.416−02	8.256−02	7.976−02	7.702−02	7.524−02	7.465−02	7.467−02	7.354−02
...									
...									
...									

et al. (2014) appear to be overestimated for at least 20% of the transitions among the lowest 78 levels of C III.

7 CONCLUSIONS

Energies for the lowest 166 levels of C III belonging to the $n \leqslant 5$ configurations have been calculated with the GRASP code. For the lowest 10 levels, discrepancies with measurements are up to 8%, but agreement is better than 1% for the remaining 156. Radiative rates are also listed for four types of transitions (E1, E2, M1 and M2) and no large discrepancies are noted for a majority of strong E1 transitions. These rates have been further employed to calculate lifetimes which are found to be in good agreement, for most levels, with other theoretical work as well as experimental values. Based on several comparisons, including the velocity and length ratios, our results for radiative rates, oscillator strengths, line strengths and lifetimes are judged to be accurate to better than 20% for a majority of strong transitions.

Collision strengths are reported for resonance transitions, at energies above thresholds, to facilitate future comparisons as at present no similar data exist. However, results for the more useful parameter Υ are listed for *all* transitions among the 166 levels of C III and over a wide range of temperature up to $10^{5.9}$ K. This range of T_e should be sufficient for the modelling of a variety of plasmas, such as astrophysical and fusion. Comparisons of Υ have been made

Table 9. Comparison of Υ for the resonance transitions of C III at three temperatures. ($a\pm b \equiv a\times10^{\pm b}$). See Table 1 for level indices.

I	J		DARC			ICFT	
T_e, K		1800	90 000	450 000	1800	90 000	450 000
1	2	1.075−1	9.453−2	5.488−2	9.000−2	8.980−2	5.430−2
1	3	3.309−1	2.839−1	1.648−1	2.850−1	2.700−1	1.630−1
1	4	5.816−1	4.738−1	2.748−1	4.580−1	4.490−1	2.720−1
1	5	3.036+0	4.035+0	5.929+0	3.000+0	3.920+0	5.860+0
1	6	5.310−3	2.780−3	1.428−3	4.020−3	2.980−3	1.500−3
1	7	1.636−2	8.342−3	4.280−3	1.230−2	8.940−3	4.510−3
1	8	2.879−2	1.395−2	7.156−3	2.000−2	1.490−2	7.520−3
1	9	2.689−1	3.465−1	3.121−1	2.680−1	3.190−1	2.950−1
1	10	5.194−2	7.897−2	7.468−2	7.070−2	7.520−2	7.290−2
1	11	2.298−1	1.090−1	4.244−2	2.950−1	1.160−1	4.340−2
1	12	3.059−1	2.616−1	3.212−1	3.050−1	2.680−1	3.220−1
1	13	1.241−2	1.237−2	6.548−3	1.650−2	1.220−2	6.420−3
1	14	4.078−2	3.968−2	2.476−2	5.290−2	3.860−2	2.320−2
1	15	6.322−2	6.231−2	3.285−2	8.360−2	6.130−2	3.210−2
1	16	1.078−1	8.499−2	1.168−1	1.280−1	8.630−2	1.200−1
1	17	3.186−2	2.946−2	1.907−2	3.330−2	2.890−2	1.830−2
1	18	5.331−2	4.916−2	3.183−2	5.590−2	4.820−2	3.050−2
1	19	7.499−2	6.872−2	4.449−2	7.740−2	6.750−2	4.260−2
1	20	1.124−1	1.434−1	2.849−1	1.260−1	1.430−1	2.820−1
1	21	5.516−3	1.793−3	7.020−4	6.260−3	1.700−3	6.850−4
1	22	1.813−2	5.444−3	2.147−3	1.940−2	5.130−3	2.070−3
1	23	3.029−2	9.091−3	3.562−3	3.300−2	8.530−3	3.420−3
1	24	4.441−2	2.159−2	1.084−2	5.510−2	2.020−2	1.020−2
1	25	8.458−2	4.426−2	4.441−2	1.060−1	4.360−2	4.520−2
1	26	4.746−2	6.652−2	8.800−2	4.780−2	5.840−2	8.310−2
1	27	7.843−3	4.494−3	2.636−3	8.730−3	3.990−3	2.360−3
1	28	2.406−2	1.348−2	7.905−3	2.630−2	1.200−2	7.120−3
1	29	4.236−2	2.268−2	1.322−2	4.350−2	2.000−2	1.180−2
1	30	1.169−2	3.011−3	2.394−3	2.050−2	2.990−3	2.310−3
1	31	9.267−3	8.622−3	5.807−3	9.530−3	7.490−3	5.220−3
1	32	1.697−2	1.457−2	9.780−3	1.610−2	1.250−2	8.770−3
1	33	2.243−2	2.046−2	1.378−2	2.230−2	1.770−2	1.230−2
1	34	1.084−2	5.740−3	3.189−3	9.910−3	5.500−3	3.070−3
1	35	1.552−2	8.202−3	4.530−3	1.400−2	7.710−3	4.300−3
1	36	1.939−2	1.026−2	5.694−3	1.770−2	9.890−3	5.510−3
1	37	3.734−2	2.516−2	2.736−2	3.330−2	2.460−2	2.730−2
1	38	5.753−3	4.493−3	2.722−3	5.940−3	3.970−3	2.350−3
1	39	9.892−3	7.475−3	4.510−3	1.010−2	6.560−3	3.880−3
1	40	1.458−2	1.023−2	6.142−3	1.400−2	9.050−3	5.310−3
1	41	3.707−2	5.159−2	1.045−1	3.890−2	4.410−2	9.340−2
1	42	2.605−2	2.665−2	3.244−2	2.390−2	2.450−2	3.000−2
1	43	9.060−3	3.404−3	1.350−3	1.010−2	3.130−3	1.240−3
1	44	4.974−4	2.978−4	1.634−4	7.050−4	2.660−4	1.530−4
1	45	1.511−3	8.960−4	4.920−4	2.140−3	7.970−4	4.590−4
1	46	2.712−3	1.513−3	8.223−4	3.600−3	1.330−3	7.670−4
1	47	5.374−3	3.090−3	3.552−3	7.680−3	2.920−3	3.260−3
1	48	6.940−3	3.717−3	1.851−3	6.710−3	3.490−3	1.760−3
1	49	1.076−2	5.240−3	2.600−3	9.600−3	4.890−3	2.470−3
1	50	1.572−2	6.772−3	3.352−3	1.240−2	6.280−3	3.170−3

with the most recent results of Fernández-Menchero et al. (2014), which are of comparable complexity and are available for a wider range of transitions and temperatures. For over one fifth of transitions, among the lowest 78 levels, the Υ of Fernández-Menchero et al. (2014) differ with our results by more than 20% and by up to a factor of 20. In most instances the Υ of Fernández-Menchero et al. (2014) are larger, consistent with the pattern found for other Be-like ions with $13 \leqslant Z \leqslant 32$ (Aggarwal & Keenan 2015).

The accuracy of our Ω and Υ data is assessed to be better than 20%, for a majority of transitions, forbidden as well as allowed. This assessment is made partly based on comparisons with available results and our experience with other Be-like ions, and mainly because: (i) we have included a large range of partial waves to achieve convergence of Ω at all energies, (ii) have included the contribution of higher neglected partial waves through a top-up, (iii) have resolved resonances in a fine energy mesh to account for their contribution, and more importantly (iv) have calculated Ω over a wide range of energy which allowed us to determine Υ

Table 9. ... continued

I	J		DARC			ICFT	
T_e, K		1800	90 000	450 000	1800	90 000	450 000
1	51	2.422−2	1.110−2	7.761−3	2.010−2	1.100−2	9.310−3
1	52	5.755−4	2.926−4	1.384−4	7.580−4	2.600−4	1.240−4
1	53	9.746−4	4.977−4	2.359−4	1.270−3	4.320−4	2.040−4
1	54	1.401−3	6.834−4	3.225−4	1.760−3	6.020−4	2.860−4
1	55	3.412−2	3.473−2	3.381−2	2.830−2	2.930−2	3.400−2
1	56	1.811−2	9.622−3	4.837−3	2.020−2	8.200−3	4.420−3
1	57	1.400−2	7.391−3	3.653−3	1.100−2	6.000−3	3.060−3
1	58	9.014−3	4.468−3	2.195−3	6.630−3	3.630−3	1.860−3
1	59	3.083−3	1.500−3	7.364−4	2.210−3	1.210−3	6.210−4
1	60	2.187−2	1.182−2	1.220−2	1.620−2	1.140−2	1.210−2
1	61	3.333−2	3.105−2	3.607−2	2.020−2	2.060−2	2.900−2
1	62	1.057−2	8.948−3	5.343−3	1.400−2	5.710−3	3.700−3
1	63	6.105−3	5.308−3	3.179−3	8.270−3	3.400−3	2.220−3
1	64	2.040−3	1.749−3	1.048−3	2.760−3	1.130−3	7.310−4
1	65	7.394−3	7.297−3	4.446−3	6.330−3	5.270−3	3.370−3
1	66	1.215−2	1.209−2	7.375−3	1.060−2	8.780−3	5.630−3
1	67	1.706−2	1.692−2	1.032−2	1.480−2	1.230−2	7.860−3
1	68	1.347−3	6.543−4	2.369−4	2.500−3	9.020−4	3.670−4
1	69	1.615−3	8.891−4	3.279−4	3.230−3	1.160−3	4.740−4
1	70	1.979−3	1.043−3	3.803−4	3.940−3	1.420−3	5.770−4
1	71	3.586−3	1.864−3	1.147−3	6.280−3	2.050−3	1.100−3
1	72	3.020−3	3.098−3	1.574−3	3.550−3	3.010−3	1.560−3
1	73	4.243−3	4.330−3	2.196−3	4.980−3	4.210−3	2.180−3
1	74	5.468−3	5.587−3	2.843−3	6.360−3	5.420−3	2.800−3
1	75	2.261−2	3.845−2	6.213−2	1.540−2	2.090−2	4.080−2
1	76	4.259−3	4.016−3	5.216−3	8.410−3	4.280−3	5.510−3
1	77	2.331−3	5.849−3	8.618−3	8.480−3	3.450−3	1.850−3
1	78	8.539−3	1.309−2	1.337−2	9.240−3	1.300−2	1.360−2

DARC: Present results with the DARC code
ICFT: Results of Fernández-Menchero et al. (2014) with the ICFT code

up to the highest temperature of our calculation, without any extrapolation. Hence, we see no apparent limitations in our data and hope these can be confidently applied to the modelling of plasmas. Nevertheless, scope remains for improvement, as for any calculation. This can perhaps be achieved by the inclusion of levels of the configurations with $n > 5$ in the generation of wave functions and the scattering process.

ACKNOWLEDGMENTS

KMA is thankful to AWE Aldermaston for financial support.

REFERENCES

Aggarwal K. M., Keenan F. P., 2012, Phys. Scr., 86, 055301
Aggarwal K. M., Keenan F. P., 2015, MNRAS, 447, 3849
Allard N., Artru M. A., Lanz T., Le Dourneuf M., 1990, A&A Suppl., 84, 563
Badnell N. R., 1997, J. Phys. B, 30, 1
Berrington K. A., Burke V. M., Burke P. G., Scialla S., 1989, J. Phys., B22, 665
Berrington K. A., Eissner W. B., Norrington P. H., 1995, Comput. Phys. Commun., 92, 290
Bryans P., Landi E., Savin D. W., 2009, ApJ, 691, 1540
Burgess A., Sheorey V. B., 1974, J. Phys., B7, 2403
Burgess A., Tully J. A., 1992, A&A, 254, 436
Cheng K. T., Chen M. H., 2008, Phys. Rev. A 77, 052504
Fernández-Menchero L., Del Zanna G., Badnell N.R., 2014, A&A, 566, A104
Glass R., 1983, Astrophys. Space Sci., 91, 417
Grant I. P., McKenzie B. J., Norrington P. H., Mayers D. F., Pyper N. C., 1980, Comput. Phys. Commun., 21, 207
Gu M. F., 2005, At. Data Nucl. Data Tables., 89, 267
Keenan F. P., Warren G. A., 1993, Sol. Phys., 146, 19
Kramida A., Ralchenko Yu, Reader J. NIST ASD Team 2015 NIST Atomic Spectra Database (ver. 5.2), online at `http://physics.nist.gov/asd`
Landi E., Doron R., Feldman U., Doscheck G. A., 2001, ApJ, 556, 912
Mitnik D. M., Griffin D. C., Balance C. P., Badnell N. R., 2003, J. Phys. , B36, 717
Nandi T., Bhattacharya N., Kurup M. B., Prasad K. G., 1996, Phys. Scr., 54, 179
Nussbaumer H., Storey P. J., 1978, A&A, 64, 139
Poulizac M. C., Buchet J.P., 1971, Phys. Scr., 4, 191
Poulizac M. C., Druetta M., Ceyseriat P., J. Quant. Spec. Rad. Transf., 1971, 11, 1087
Safronova U. I., Derevianko A., Safronova M. S., Johnson W. R., 1999a, J. Phys., B32, 3527
Safronova U. I., Johnson W. R., Derevianko A., 1999b, Phys. Scr., 60, 46
Stark D. P., Richard J., Siana B., Charlot S., Freeman W.

R., Gutkin J., Wofford A., Robertson B., Amanullah R., Watson D., Milvang-Jensen B., 2014, MNRAS, 445, 3200
Swings P., Struve O., 1940, Publications of the Astron. Soc. Pacific, 52, 394
Tachiev G., Froese Fischer C., 1999, J. Phys. , B32, 5805

Walborn N. R., Sota A., Apellániz, J. M., Alfaro E. J., Morrell N. I., Barbá R. H., Arias J. I., Gamen R. C., 2010, ApJ, 711, Ll43